Unidirectional block between isolated rabbit ventricular cells coupled by a variable resistance

Ronald W. Joyner, Hiroki Sugiura, and Rosemarie C. Tan
Todd Franklin Cardiac Research Laboratory, The Children's Heart Center, Department of Pediatrics, Emory University, Atlanta, Georgia, 30323

ABSTRACT We have used pairs of electrically coupled cardiac cells to investigate the dependence of successful conduction of an action potential on three components of the conduction process: (a) the amount of depolarization required to be produced in the nonstimulated cell (the "sink" for current flow) to initiate an action potential in the nonstimulated cell, (b) the intercellular resistance as the path for intercellular current flow, and (c) the ability of the stimulated cell to maintain a high membrane potential to serve as the "source" of current during the conduction process. We present data from eight pairs of simultaneously recorded rabbit ventricular cells, with the two cells of each pair physically separated from each other. We used an electronic circuit to pass currents into and out of each cell such that these currents produced the effects of any desired level of intercellular resistance. The cells of equal size (as assessed by their current threshold and their input resistance for small depolarizations) show bidirectional failure of conduction at very high values of intercellular resistance which then converts to successful bidirectional conduction at lower values of intercellular resistance. For cell pairs with asymmetrical cell sizes, there is a large range of values of intercellular resistance over which unidirectional block occurs with conduction successful from the larger cell to the smaller cell but with conduction block from the smaller cell to the larger cell. We then further show that one important component which limits the conduction process is the large early repolarization which occurs in the stimulated cell during the process of conduction, a process that we term "source loading."

INTRODUCTION

It has been appreciated for many years that initiation of cardiac arrhythmias occurs in some situations as a reentrant pathway on the basis of slow conduction and unidirectional block (UB) of a propagating cardiac action potential (see review by Durrer et al., 1978). Experimental studies demonstrating UB in the intact heart have focused on ventricular ischemia (Janse et al., 1985; Lazzara, 1988; Lazzara and Scherlag, 1988; Reddy and Lynch, 1978) or on normal ventricular myocardium (Hamamoto et al., 1987; Chen et al., 1988; Frazier et al. 1989). Other studies have focused on UB in the normal or diseased atrioventricular node (Moe et al., 1956, 1965; Barold et al. 1977; Salernao et al., 1979; Mazgelev et al., 1981; Watanabe, 1981; Lin et al., 1985; Mahmoud et al., 1985; Okumura et al., 1985; Kim et al., 1987). It has been difficult from these studies on the intact heart to ascertain either the mechanisms producing UB or the exact location(s) at which UB occurs. A variety of in vitro experimental models have been developed to study UB. De la Fuente et al. (1971) produced UB by cutting atrial tissue into a small region connected to a large region by a narrow isthmus. In this case, a rate-dependent UB could be demonstrated with preferential conduction from the large region to the small region. UB was also demonstrated in Purkinje strands with depressed conduction (Cranefield et al., 1971; Wald et al., 1980; Waxman et al., 1980) in diseased human ventricular myocardium (Gilmour et al., 1983), or in an isolated ventricular sheet (Kamiyama et al., 1986). In isolated atrial tissue, UB has been shown to be of fundamental importance in the initiation of supraventricular tachycardia by premature beats (Allessie et al., 1975, 1976; Bonke et al., 1975) and similar studies have been conducted to develop ventricular reentry around a fixed barrier (Bernstein and Frame, 1990). We showed (Overholt et al., 1984) that UB was present over most regions of the canine ventricular subendocardium such that conduction from the ventricular muscle cells to the overlying Purkinje cells could occur at many regions for which conduction from Purkinje cells to the ventricular muscle cells was blocked.

UB has also been studied in theoretical models of action potential conduction. We presented (Joyner, 1981; Joyner et al., 1984*b*) studies with a one-dimensional cardiac strand in which we showed that spatial inhomogeneities in either the radius of the strand or of the intercellular coupling resistance could produce UB. We also presented (Joyner et al., 1984*a*) a theoretical model of two inhomogeneously coupled cardiac tissue layers to explain our experimental results showing UB

Address correspondence and reprint requests to Dr. Ronald W. Joyner, Department of Pediatrics, Emory University School of Medicine, 2040 Ridgewood Drive, NE, Atlanta, GA 30322.

0006-3495/91/11/1038/08 $2.00

between Purkinje and ventricular muscle cells. Other models have been developed in which UB could be demonstrated by inserting premature stimuli into a system of cells with different refractory periods or regional conduction delay (Smith and Cohen, 1984; Lesh et al., 1989; Quan and Rudy, 1990).

The quantitative uncertainties of the membrane models used for these theoretical studies and the geometrical complexities of previous experimental studies led us to develop a simpler experimental model system in which the location of the UB could be precisely determined and the electrical properties of the tissue on each side of this UB site could be directly measured. We have accomplished this by studying pairs of isolated rabbit ventricular cells that are not actually touching each other and thus have no direct pathway for intercellular current flow. We devised an electronic circuit (Tan and Joyner, 1990) that provides the electrical coupling between the cells in order to directly test the influence of geometrical factors on the production of UB. In the previous publication (Tan and Joyner, 1990) we used the circuit to couple a single cell to a passive RC circuit. In this work we use simultaneous recordings from two isolated cells to study the effects of coupling resistance on action potential properties and the success or failure of action potential conduction.

METHODS

I. Cell Isolation

Adult rabbits of either sex weighing 1–1.5 kg were anesthetized using 50 mg/kg Nembutal i.v. and 1,000 U heparin. The heart was rapidly excised and the aorta cannulated for Langendorff perfusion and isolation of single cells according to the methods described in detail in our recent publication (Tan and Joyner, 1990). Briefly, the heart was first perfused at a rate of 4 ml/min per g with a nominally Ca^{2+}-free Tyrode's solution of the following mM composition: NaCl, 100; KCl, 10; $MgSO_4$, 5; KH_2PO_4, 1.2; Taurine, 50; Dextrose, 20; and Hepes, 10 with pH adjusted to 7.2 using NaOH. After the blood was washed from the coronary arteries, the heart was perfused with the same Tyrode's solution containing Type I collagenase (Sigma Chemical Co., St. Louis, MO; 13.3 mg/100 cc) and Type XIV protease (Sigma Chemical Co.; 6.6 mg/100 cc) for 5–15 min. The collagenase was then washed from the heart with a high K^+/low Cl^- storage solution of the following mM composition: potassium glutamate, 140; $MgCl_2$, 5; EGTA, 11; Dextrose, 10; and Hepes, 10 with pH adjusted to 7.4 using KOH. After perfusion of the high K^+ storage solution, the left ventricle was opened and small pieces of left ventricular endocardium were removed and gently agitated in the high K^+ storage solution. The isolated cells were transferred to an experimental chamber containing (in mM) NaCl (148), KCl (4), $CaCl_2$ (1.8), $MgCl_2$ (0.5), NaH_2PO_4 (0.3), dextrose (5), Hepes (5) with the pH adjusted to 7.4 using NaOH. The chamber was continuously perfused with this solution at 2 cc/min at room temperature or at 36°C as noted.

Only those cells that were quiescent with preservation of their rod-shaped appearance were studied using relatively high resistance patch pipettes in order to minimize intracellular dialysis. The electrodes were pulled from borosilicate glass and after fire polishing, had resistances of 4–7 Mohms when filled with the following internal solution (mM): KCl, 120; Na_2CrP,5; MgATP, 5; EGTA, 11; Hepes, 10 with pH adjusted to 7.2 using KOH. High resistance seals were formed with the cell membrane using light suction, which was then followed by disruption of the cell membrane with transient suction.

II. Electrical coupling of a pair of cells

We have developed an electronic circuit that can provide a variable effective coupling resistance between two isolated heart cells which are not actually in direct contact with each other (Tan and Joyner, 1990). If V_1 is the time-varying membrane potential (volts) of cell 1 and V_2 is the time-varying membrane potential of cell 2, and if the two cells were actually coupled by an intercellular resistance R_c (ohms), then there would be a time-varying current I_c (amps) flowing from cell 1 to cell 2 (positive or negative) given by $I_c = (V_1 - V_2)/R_c$. In brief, our circuit consists of two amplifiers that continuously compute $(V_2 - V_1)$ and $(V_1 - V_2)$, respectively. The outputs of these amplifiers go through voltage to current (Vto I) Converters and then back to the cells to provide the identical current inputs to cell 1 and model cell 2 that would have been conducted across a real intercellular resistance R_c. The specification of the value of R_c is a combination of the fixed gain of the V to I converters and a variable gain of the two amplifiers, giving us control of the coupling resistances in our experiments. Periodic stimuli are added to the current input of the stimulated cell as current pulses of 2 ms duration and amplitude 5-10% suprathreshold for activation of the stimulated cell (1.0–2.5 nA) at a frequency of 1 Hz. Simultaneous recordings from each cell were made with an Axoclamp 2A (Axon Instruments, Inc.) dual preamplifier in the current clamp mode, using the internal V to I converters to feedback the desired currents to each headstage from the coupling circuit. Data was sampled either directly into a microcomputer, using pClamp or Axotape software (Axon Instruments, Inc.), or was recorded continuously with a VCR based A/D converter system (Medical Systems Corp.) at a sample rate of 22 kHz/channel. Series resistance for the recordings of each cell were carefully compensated by internal bridge balance adjustments for each electrode after recording of the membrane potential of each cell was established.

In the following sections we refer to the "size" of the two cells of a cell pair. We did not attempt to measure the cell size by histologic techniques, but we use this term to indicate the electrical load of the cell. If all cells had identical membrane properties, then the cell size, as measured in cm^2 of membrane, would be inversely proportional to the input resistance and directly proportional to the current threshold. The irregular shape of the cells precludes a quantitative measurement of membrane area by photomicrographs. The input resistance of the cell is known to show rectification, even for small changes in membrane potential. We have defined the input resistance, R_{in}, for our cells as the voltage response produced by a small current pulse (0.1–0.3 nA) of duration 20 ms, divided by the amplitude of the current. For these measurements, we used membrane depolarizations less than 10 mV from the resting membrane potential. To measure the current threshold, I_{th}, we used repetitive current pulses of 2 ms duration at 1 Hz (for experiments at room temperature) or 2 Hz (for experiments at 36°C) starting with suprathreshold current magnitudes and slowly reducing the current magnitude until failure of activation occurred.

RESULTS

A total of eight cell pairs were studied. We present here the results from two pairs of cardiac cells. These cell pairs were chosen as a nearly symmetrical cell pair

(experiment 3 in Table 1) and an asymmetrical cell pair (experiment 2 in Table 1) in which the cell size differs by a factor of nearly two. Results from the other six cell pairs were consistent with these results. The basic data on these two cell pairs were obtained without cell coupling (see Fig. 1). Thus, for the symmetrical cell pair the values of R_{in} and I_{th} are nearly the same for cell 1 and cell 2, while for the asymmetrical cell pair it is clear that cell 1 is smaller than cell 2 by a factor of about two on the basis of the lower I_{th} and higher R_{in}.

We first present results (Figs. 2–3) for the nearly symmetrical cell pair. Fig. 2*A* shows the simultaneous recordings from cell 1 (*solid line*) and cell 2 (*dotted line*) under conditions where there is no electrical coupling between the two cells. The top panel illustrates the action potential (AP) response of cell 1 while the lower panel shows the AP response of cell 2. The resting membrane potential (RMP) was −80 and −81 mV for cell 1 and cell 2, respectively. The action potential duration (APD) for the two cells is between 400–450 ms with cell 2 having a lower early plateau than cell 1. The peak amplitudes are +48 mV for cell 1 and +52 mV for cell 2.

In Fig. 2*B*, we show the results obtained when we coupled the cells with an effective R_c of 400 Mohm. Stimulation of cell 1 (*upper*) produces a cell 1 AP that is slightly decreased in amplitude (cf. Fig. 2*A*) but markedly decreased in APD. Cell 2 has a response of only ~20 mV amplitude. For stimulation of cell 2 (Fig. 2*B*, *lower*), cell 2 also has an AP with slightly lowered amplitude and a markedly decreased APD. The AP responses of cell 1 when stimulated (*upper*) and cell 2 when stimulated (*lower*) are slightly different, reflecting the different intrinsic plateau properties as shown in Fig. 2*A*. The overall result is that, with an R_c of 400 Mohm, there is bidirectional block of conduction, a large, nearly symmetrical APD reduction for the stimulated cell, and responses of only 15–20 mV amplitude in the unstimulated cell.

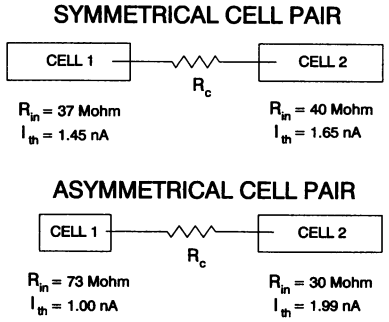

FIGURE 1 Diagram of two cardiac cell pairs with parameters input resistance (R_{in}), and current threshold (I_{th}) as indicated for each cell.

When we lowered the effective R_c to 300 Mohm, we obtained the results displayed in Fig. 3*A*. For stimulation of cell 1 (*upper*) the AP of cell 1 has a rapid early repolarization which is interrupted by the activation of cell 2. After cell 2 is activated, cell 1 and cell 2 maintain very similar membrane voltages throughout the rest of the AP waveforms, with nearly simultaneous termination. The lower panel of Fig. 3*A* shows the results for stimulation of cell 2. For the stimulation of cell 2 there is a rapid early repolarization of cell 2 which is then interrupted by the activation of cell 1. After the activation of cell 1, the response of cell 2 rises to nearly equal the plateau level of cell 1 and, as in the upper panel of Fig. 3*A* (for stimulation of cell 1), the two APs have nearly simultaneous termination. There is a slight asymmetry in the AP responses for stimulation of cell 1 (*upper*) and stimulation of cell 2 (*lower*) as illustrated at a faster time base in Fig. 3*B*. The latency between cell 1 and cell 2 (*upper*) is 19 ms while the latency between cell

TABLE 1 Relationship between current threshold, input resistance and critical coupling resistance for pairs of isolated rabbit ventricular cells

		I_{TH} (nA)			R_{in} (Mohm)			Critical resistance (Mohm)		
Experiment	Name	Cell 1	Cell 2	Ratio (2)/(1)	Cell 1	Cell 2	Ratio (1)/(2)	(2) to (1)	(1) to (2)	Ratio
1	1016-2	1.19	1.59	1.34	60	27	2.2	500	200	2.5
2	1016-5	1.00	1.99	1.99	73	30	2.4	500	120	4.17
3	1106-3	1.45	1.65	1.14	37	40	0.93	300	300	1.0
4	1106-2	1.30	1.45	1.12	43	43	1.0	300	250	1.20
5	0410-2	1.15	1.3	1.13	44	32	1.4	303	217	1.40
6	0410-5	1.75	2.0	1.14	30	23	1.3	238	139	1.71
7	0416-4	1.56	2.03	1.30	34	22	1.6	222	108	2.06
8	0417-1	1.86	2.02	1.09	22	21	1.05	167	123	1.36
Mean ± SD				1.26 ± 0.3			1.45 ± .55			1.87 ± 1.0*

*$P < 0.05$, comparing the critical resistance ratio to the ratio of current thresholds or to the ratio of input resistances. Note: the two cells of a cell pair were defined as "cell 1" or "cell 2" such that the I_{thresh} of cell 2 was larger than cell 1. Experiments 1–4 were done at room temperature, experiments 5–8 were done at 36°C.

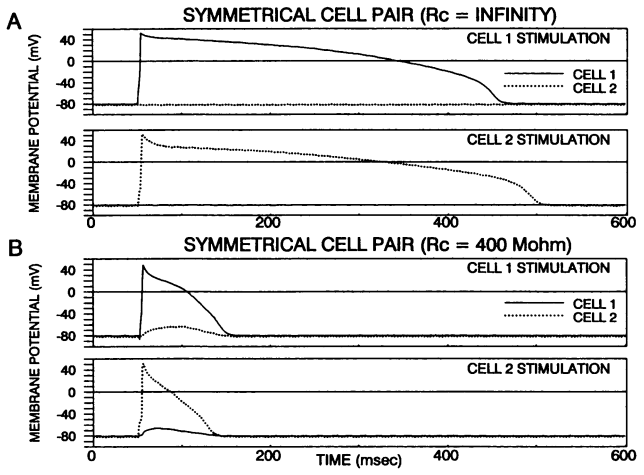

FIGURE 2 (*A*) Results from symmetrical cell pair, completely uncoupled. (*upper*) Simultaneous recording from cell 1 (*solid line*) and cell 2 (*dotted line*) for stimulation of cell 1. (*lower*) Simultaneous recording from cell 1 (*solid line*) and cell 2 (*dotted line*) for stimulation of cell 2. (*B*) Results from symmetrical cell pair; coupling resistance (R_c) is 400 Mohm. (*upper*) Simultaneous recording from cell 1 (*solid line*) and cell 2 (*dotted line*) for stimulation of cell 1. (*lower*) Simultaneous recording from cell 1 (*solid line*) and cell 2 (*dotted line*) for stimulation of cell 2.

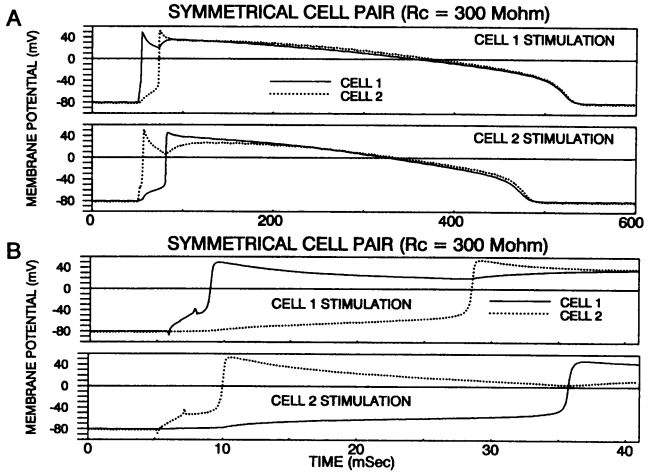

FIGURE 3 (*A*) Results from symmetrical cell pair, R_c is 300 Mohm. (*upper*) Simultaneous recording from cell 1 (*solid line*) and cell 2 (*dotted line*) for stimulation of cell 1. (*lower*) Simultaneous recording from cell 1 (*solid line*) and cell 2 (*dotted line*) for stimulation of cell 2. (*B*) Results from symmetrical cell pair, R_c is 300 Mohm. (*upper*) Simultaneous recording from cell 1 (*solid line*) and cell 2 (*dotted line*) for stimulation of cell 1. (*lower*) Simultaneous recording from cell 1 (*solid line*) and cell 2 (*dotted line*) for stimulation of cell 2. Data here is the same as for *A*, but showing only the initial portion of the data at a faster time base.

2 and cell 1 (*lower*) is 26 ms. The extent of the rapid early repolarization is somewhat greater for cell 2 stimulation than for cell 1 stimulation. Overall, the results for R_c of 300 Mohm show bidirectional conduction with similar values for APD and latency.

Data for the second pair of cells (asymmetrical cell pair) are shown in Figs. 4–6. Fig. 4 *A* illustrates the responses of cell 1 (*upper*) and cell 2 (*lower*) when the two cells are completely uncoupled. The RMP of both cells is −80 mV. Cell 2 has a higher peak amplitude (+56 mV vs. +47 mV), a higher plateau amplitude, and a longer APD than cell 1. Fig. 4 *B* shows the results obtained when we coupled these two cells with an effective coupling resistance of 1,000 Mohm. For cell 1 stimulation (*upper*) and for cell 2 stimulation (*lower*) there is a marked decrease in the APD of the stimulated cell and bidirectional conduction failure. The passive response of cell 2 (*upper*) is smaller than the passive response of cell 1 (*lower*) as would be expected from the higher input resistance of cell 1.

When we reduced the effective R_c to 500 Mohm, we got the results shown in Fig. 5 *A*. In the upper panel (cell 1 stimulation) the cell 1 AP is further reduced in APD (cf. Fig. 4 *B*) and a larger passive response occurs in cell 2, but conduction does not occur. In contrast, the lower panel (cell 2 stimulation) shows an AP in cell 2 with a slight early repolarization interrupted by activation of cell 1. After activation of cell 1, the two cells maintain nearly equal plateau values and terminate nearly simul-

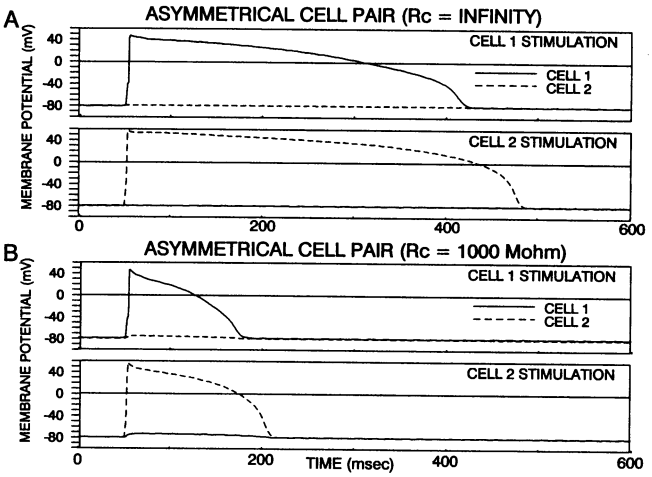

FIGURE 4 (*A*) Results from asymmetrical cell pair, completely uncoupled. (*upper*) Simultaneous recording from cell 1 (*solid line*) and cell 2 (*dashed line*) for stimulation of cell 1. (*lower*) Simultaneous recording from cell 1(*solid line*) and cell 2 (*dashed line*) for stimulation of cell 2. (*B*) Results from asymmetrical cell pair, R_c is 1,000 Mohm. (*upper*) Simultaneous recording from cell 1 (*solid line*) and cell 2 (*dashed line*) for stimulation by cell 1. (*lower*) Simultaneous recording from cell 1 (*solid line*) and cell 2 (*dashed line*) for stimulation of cell 2.

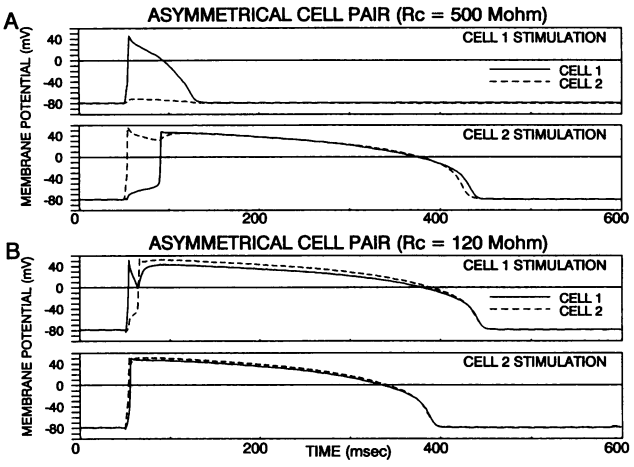

FIGURE 5 (*A*) Results from asymmetrical cell pair, R_c is 500 Mohm. (*upper*) Simultaneous recording from cell 1 (*solid line*) and cell 2 (*dashed line*) for stimulation of cell 1. (*lower*) Simultaneous recording from cell 1 (*solid line*) and cell 2 (*dashed line*) for stimulation of cell 2. (*B*) Results from asymmetrical cell pair, R_c is 120 Mohm. (*upper*) Simultaneous recording from cell 1 (*solid line*) and cell 2 (*dashed line*) for stimulation of cell 1. (*lower*) Simultaneous recording from cell 1 (*solid line*) and cell 2 (*dashed line*) for stimulation of cell 2.

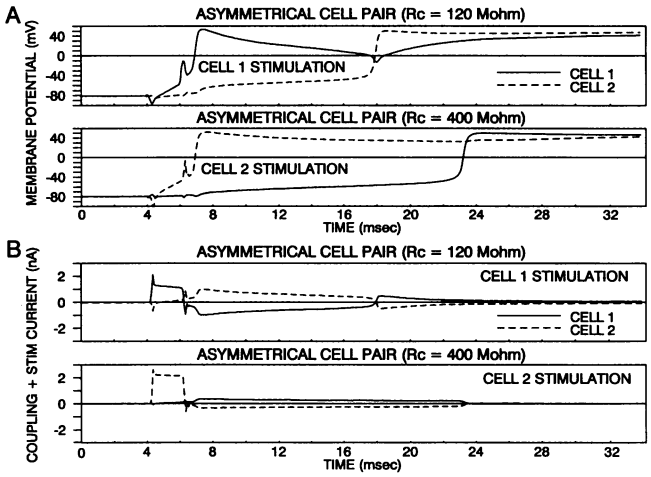

FIGURE 6 (*A*) Results from asymmetrical cell pair: (*upper*) R_c is 120 Mohm. Simultaneous recording from cell 1 (*solid line*) and cell 2 (*dashed line*) for stimulation of cell 1. (*lower*) R_c is 400 Mohm. Simultaneous recording from cell 1 (*solid line*) and cell 2 (*dashed line*) for stimulation of cell 2. (*B*) Results from asymmetrical cell pair: (*upper*) R_c is 120 Mohm. Simultaneous recording for stimulation of cell 1 of the coupling and stimulus current for cell 1 (*solid line*) and the coupling current for cell 2 (*dashed line*). (*lower*) R_c is 400 Mohm. Simultaneous recording for the stimulation of cell 2 of the coupling current for cell 1 (*solid line*) and the coupling and stimulus current for cell 2 (*dashed line*).

taneously. The overall result is a clear demonstration of unidierctional block of conduction, with conduction from cell 1 to cell 2 blocked while conduction from cell 2 to cell 1 is successful.

We continued to reduce the effective R_c, testing for conduction from cell 1 to cell 2. For effective R_c values of 400, 250, 200, 180, 160, and 140 Mohm unidirectional block of conduction was maintained. However, when we further reduced the effective coupling resistance to 120 Mohm we obtained the results shown in Figure 5 *B*. For stimulation of cell 1 (*upper*) there is a cell 1 AP with a large extent of early repolarization that is interrupted by activation of cell 2. Even after cell 2 activates, there is a maintained difference in plateau amplitude of 10–15 mV but nearly simultaneous AP termination. For cell 2 stimulation (*lower*) the latency between cell 2 activation and cell 1 activation is now very short (5 ms) and the two APs are nearly identical.

One important difference in the conduction process from cell 1 to cell 2, compared with the conduction process from cell 2 to cell 1, is the extent of the early partial repolarization caused by the current flow from the stimulated cell to the nonstimulated cell in the time interval between the two activation times. We illustrate this difference more clearly in Figure 6 *A* and *B*. Fig. 5 *A* showed conduction from cell 2 to cell 1 of the asymmetrical cell pair with a coupling resistance as high as 500 Mohm but with a latency of 30 ms. When we lowered R_c to 400 Mohm, the latency from cell 2 to cell 1 was decreased to 18 ms, as shown in the lower panel of Fig. 6 *A*. The upper panel of Fig. 6 *A* shows the conduction from cell 1 to cell 2 at R_c of 120 Mohm (as in the top panel of Fig. 6 *A*). When we compare the conduction process for cell 1 to cell 2 at R_c of 120 Mohm (*top*) to the conduction process for cell 2 to cell 1 at R_c of 400 Mohm (*bottom*), it is clear that the peak amplitudes of the APs in the stimulated cells are only slightly decreased from the values for complete uncoupling (cf. Fig. 4 *A*), but the early repolarization causes a drop of potential in cell 1 (*upper*) by nearly 50 mV, while for cell 2 (*lower*) the early repolarization causes a drop of potential in cell 2 of only 15 mV. Therefore, during the time interval over which the nonstimulated cell is being depolarized by current from the stimulated cell, the membrane potential of the sitmulated cell is strongly decreased when conduction occurs from cell 1 to cell 2, while for conduction from cell 2 to cell 1 the membrane potential of the stimulated cell is maintained at a higher level. The driving force for current flow across the intercellular resistance is equal to the potential difference between the stimulated cell and the nonstimulated cell. At the time just before activation of the nonstimulated cell, this potential difference for conduction from cell 2 to cell 1 (*bottom*) is nearly twice as large (~80 mV) as for conduction from cell 1 to cell 2 (~40 mV). The effect of

this drop in the potential difference is seen very clearly in Fig. 6 *B* where we plot the coupling current for cell 1 and cell 2 with R_c = 120 Mohm (cell 1 stimulation, *upper*) and with R_c = 400 Mohm (cell 2 stimulation, *lower*). The currents recorded here represent the currents actually supplied through the pipettes by our coupling circuit. This current includes the stimulus current for cell 1 in the upper panel and the stimulus current for cell 2 in the lower panel. Notice that the coupling current is much larger for the upper panel during the conduction process, because the larger cell 2 requires more current for activation. During the process of conduction this current declines in magnitude by nearly 50%. For conduction from cell 2 to cell 1 (*lower*) the coupling current is smaller and nearly constant during the conduction process. This effect of the coupling current to produce a lowering of the ampliutde of the potential in the stimulated cell which is the source of current flow for conduction could be described as "source loading." Comparing Fig. 6 *A* for conduction between cells of different sizes, to Fig. 3 *B*, for conduction between cells of similar sizes, we see that the extent of this "source loading" is very asymmetrical for Fig. 6 *A* and nearly symmetrical for Fig. 3 *B*.

Results from all eight cell pairs are summarized in Table 1. Experiments 1–4 were done at room temperature, while experiments 5–8 were done at 36°C. We have identified the two cells in each pair as "cell 1" or "cell 2" on the basis of the measured current threshold for each cell, with the current threshold for cell 2 being larger and thus indicating that the mean ratio of cell size for cell 2 compared with cell 1 was 1.26 ± 0.3, using current threshold as the sole indicator of cell size. When we assessed the relative cell size by measurements of the ratio of R_{in} for each cell of a pair, the mean values for relative cell size were 1.45 ± 0.55. For each cell pair we also measured the critical coupling resistance above which conduction failed from cell 2 to cell 1 and the critical coupling resistance above which conduction failed from cell 1 to cell 2. The mean value for the ratio of these critical coupling resistances was 1.87 ± 1.0, significantly higher than the ratio of cell size as determined by the ratio of current thresholds or as determined by the raito of input resistances. We also evaluated the extent of the "source loading" in each of the eight cell pairs of Table 1 by measuring the decline in potential for the stimulated cell from the action potential peak to the minimal value just before the action potential was initiated in the unstimulated cell. For conduction at the critical value of R_c, there was a 33 ± 12 mV decline in the membrane potential when the larger cell was stimulated and a 49 ± 16 mV decline in the membrane potential when the smaller cell was stimulated ($P < 0.05$).

DISCUSSION

Our studies on pairs of cardiac cells complement many recent studies on physically connected cell pairs. Weingart and Maurer (1988) showed AP conduction between rat ventricular cells with a measured intercellular resistance as high as 375 Mohm, although the "normal" value of intercellular resistance coupling is apparently much lower. Conduction between two cardiac cells clearly involves three major components: (*a*) the amount of depolarization required in the nonstimulated cell (the "sink" for current flow) to initiate an AP in the nonstimulated cell, (*b*) the intercellular resistance as the path for intercellular current flow, and (*c*) the ability of the stimulated cell to maintain a high membrane potential to serve as the "source" of current for the nonstimulated cell.

Our experiments allowed us to make some determination of the ways in which these three components determine conduction success or failure. With regard to the first component, the voltage threshold of the nonstimulated cell, one can see from our Figs. 3 *B* and 6 *A* that the voltage threshold for each cell when it acts as the "sink" (the nonstimulated cell) is very nearly the same as when that same cell is directly stimulated. Thus, this component represents a relatively fixed value for the conduction process. The second ocmponent, the intercellular resistance, is under direct experimental control with our technique. The third component, the amplitude of the membrane potential in the stimulated cell during conduction, was shown to be largely dependent on the direction of conduction in the case for the asymmetrical cell pair. If one assumes that the voltage threshold of the nonstimulated cell remains constant (as we have shown) and if one also assumes, for simplicity, that the amplitude of the membrane potential of the stimulated cell remains constant during the conduction process (which is not the case), then one can derive a simple relationship for how the critical R_c (above which conduction would fail) would vary with the direction of conduction between two cells of different membrane areas. Let A_1 be the membrane area of cell 1 and A_2 be the membrane area of cell 2. Let R_m be the specific resistivity (ohm-cm^2) of each cell in the voltage range just below the voltage threshold, V_{th}. Under these conditions, if V_p were the constant potential of the stimulated cell during the conduction process, then we can let $R_c(1,2)$ be the critical R_c for conduction from cell 1 to cell 2 and R_c (2,1) be the critical R_c for conduction from cell 2 to cell 1 and we can derive the following relationship:

$$V_{th} = [V_p R_m/A_2]/[R_c(1, 2) + R_m/A_2]$$
$$= [V_p R_m/A_1]/[R_c(2, 1) + R_m/A_1],$$

where V_{th} and V_p are expressed with respect to the RMP. This expression treats the combination of the two cells and the intercellular resistance as a voltage divider circuit. The net result would be that $R_c(2, 1)/R_c(1, 2) = A_2/A_1$. However, our data show that this relationship cannot account entirely for the measured difference in $R_c(1, 2)$ and $R_c(2, 1)$ for the asymmetrical cell pair. For our asymmetrical cell pair, it is clear that A_2/A_1 is ~ 2 as estimated from the differences in R_{in} or I_{th}; yet, the ratio of $R_c(2, 1)$ to $R_c(1, 2)$ is 500/120 or ~ 4. If we now include in the analysis the decline in V_p (to ~ 70 mV) for the stimulated cell 1 during conduction from cell 1 to cell 2 and the decline in V_p (to ~ 125 mV) for the stimulated cell 2 during conduction from cell 2 to cell 1, there is nearly a twofold difference in V_p for the asymmetrical cell pair depending on the direction of stimulation. This larger reduction in V_p for the stimulated cell 1 due to the enhanced "source loading" of a large cell (cell 2) onto a smaller cell (cell 1) leads to a further lowering of the value of $R_c(1, 2)$ which then produces a larger increase in the ratio $R_c(2, 1)/R_c(1, 2)$ than was accounted for by the analysis with a constant V_p. Therefore, the actual asymmetry in $R_c(2, 1)$ and $R_c(1, 2)$ for asymmetrical cell pairs is strongly affected by the "source loading" phenomenon. From a similar analysis, one can show that a difference in the peak amplitude for cell 1 versus cell 2 would have little effect on the values of $R_c(1, 2)$ and $R_c(2, 1)$. From our data on the asymmetrical cell pair, the maximum amplitudes of the action potentials when uncoupled (measured from the resting potential) were 127 mV for cell 1 and 136 mV for cell 2. These differences would account for only a 7% difference in $R_c(1, 2)$ and $R_c(2, 1)$. The data from all eight cell pairs presented in Table 1 allowed a statistical test of the hypothesis that the degree of asymmetry of conduction, expressed as $[R_c(2, 1)/R_c(1, 2)]$, was greater than the asymmetry of input resistance or of current threshold.

The rapid early repolarization is apparent in the symmetrical cell pair (Fig. 3 *B*) as well as in the asymmetrical cell pair (Fig. 6 *A*). It is important to note that this "source loading" does not significantly lower the peak amplitude of the stimulated cell (which occurs when the cell membrane sodium conductance is high) but exerts its effect immediately after the peak of the AP (when the depolarization is supported by a combination of conductances much lower than the maximum sodium conductance). Another feature of "source loading" that is particularly apparent in Fig. 3 *B* for the nearly symmetrical cell pair is that the process is progressive during the period of conduction. This process then limits the maximum delay that can be obtained between two coupled cells. However, this process is partly counteracted by a process in the nonstimulated cell characterized by a continuous rise in membrane potential over the latency period even though the source membrane potential is continuing to decrease. Therefore, the overall process of conduction between cells coupled by relatively high resistance depends on membrane conductance changes in the subthreshold voltage range for the nonstimulated cells, as well as on the membrane conductance changes in the stimulated cell that occur after the initial rapid increase in sodium conductance. These phenomena suggest that conduction among cardiac regions with relatively high intercellular coupling may be strongly affected by alterations in membrane conductances other than the sodium conductance.

We have deliberately produced a simplified system of two cardiac cells to study the effects of intercellular coupling resistance on action potential propagation in order to be able to quantitatively measure the cell size and action potential properties of each cell. Conduction in the intact cardiac syncytium varies from being a nearly continuous process (through cells with low resistance coupling) in some regions to being clearly discontinuous at some locations in the normal heart and in ischemic regions. It is important to note that the cell pairs we are studying are coupled at much higher resistances than would be expected between a pair of cells within the cardiac syncytium at regions of rapid conduction. We have developed this model system to study conduction at regions where significant conduction delays occur. Our model specifically excludes the possible influence of voltage changes or ionic changes in narrow extracellular clefts that may occur in the intact cardiac syncytium, including only a resistive connection between cells (Hellam and Studt, 1974; Pressler, 1984). Extracellular recordings and intracellular recordings (Ursell et al., 1985; Kienzle et al., 1987) show that conduction in ischemic tissue is a process of sequential activation of small groups of cells, with nearly synchronous activation of the cells within each group. Our results suggest that the size of the groups of cells and the activation sequence of the groups may strongly determine the presence or absence of conduction block with ischemic tissue.

This work was supported in part by National Institutes of Health grants HL-22562, HL-41851, and HL-27385, and the Children's Research Center.

Received for publication 5 February 1991 and in final form 2 July 1991.

REFERENCES

Allessie, M. A., F. I. Bonke, and F. J. Schopman. 1975. The mechanism of supraventricular tachycardia induced by a single premature beat in the isolated left atrium of the rabbit. I. Circus movement as a consequence of unidirectional block of the premature impulse. *Recent Adv. Stud. Card. Struct. Metab.* 5:303–308.

Allessie, M. A., F. I. Bonke, and F. J. Schopman. 1976. Circus

movement in rabbit atrial muscle as a mechanism of tachycardia. II. The role of nonuniform recovery of excitability in the occurrence of unidirectional block, as studied with multiple microelectrodes. *Circ. Res.* 39:168–177.

Barold, S. S., M. B. Fracp, and P. Coumel. 1977. Mechanisms of atrioventricular junctional tachycardia. Role of reentry and concealed accessory bypass tracts. *Am. J. Cardiol.* 39:97–106.

Bernstein, R. C., and L. H. Frame. 1990. Ventricular reentry around a fixed barrier. Resetting with advancement in an *in vitro* model. *Circulation.* 81:267–280.

Bonke, F. I., M. A. Allessie, and L. N. Bouman. 1975. Reentry in the atrium *Bull. Schweiz. Akad. Med. Wiss.* 31:33–44.

Chen, P. S., P. D. Wolf, E. G. Dixon, N. D. Danieley, D. W. Frazier, W. M. Smith, and R. E. Ideker. 1988. Mechanism of ventricular vulnerability to single premature stimuli in open-chest dogs. *Circ. Res.* 62:1191–1209.

Cranefield, P. F., H. O. Klein, and B. Hoffmann. 1971. Conduction of the cardiac impulse. I. Delay, block, and one-way block in depressed Purkinje fibers. *Circ. Res.* 28:199–219.

De La Fuente, D., B. I. Sasnyiuk, and G. K. Moe. 1971. Conduction through a narrow isthmus in isolated canine atrial tissue. *Circulation.* 46:803–821.

Durrer, D., K. I. Lie, M. J. Janse, and R. M. Schuilenburg. 1978. Mechanisms of tachyarrhythmias, past and present. *Eur. J. Cardiol.* 88:281–297.

Frazier, D. W., P. D. Wolf, J. M. Wharton, A. S. Tang, W. M. Smith, and R. E. Ideker. 1989. Stimulus-induced critical point. Mechanism for electrical initiation of reentry in normal canine myocardium. *J. Clin. Invest.* 83:1039–1052.

Gilmour, R. F., J. J. Heger, E. N. Prystowsky, and D. P. Zipes. 1983. Cellular electrophysiologic abnormalities of diseased human ventricular myocardium. *Am. J. Cardiol.* 51:137–144.

Hamamoto, H., E. Kinoshita, H. Tomoda, and Y. Goto. 1987. The evidence of transmural unidirectional block by experimental current induced ventricular tachycardia in the canine heart. *Jpn. Circ. J.* 51:181–187.

Hellam, D. C., and J. W. Studt. 1974. Linear analysis of membrane conductance and capacitance in cardiac purkinje fibres. *J. Physiol.* 243:661–694.

Janse, M. J., A. Capucci, R. Coronel., and M. A. Fabius. 1985. Variability of recovery of excitability in the normal canine and the ischaemic porcine heart. *Eur. Heart J.* 6 (Supp):41–52.

Joyner, R. W. 1981. Mechanisms of unidirectional block in cardiac tissues. *Biophys. J.* 35:113–125.

Joyner, R. W., E. D. Overholt, B. Ramza, and R. D. Veenstra. 1984. Propagation through electrically coupled cells: two inhomogeneously coupled cardiac tissue layers. *Am. J. Physiol.* 247:H596–609.

Joyner, R. W., R. D. Veenstra, D. Rawling and A. Chorro. 1984. Propagation through electically coupled cells. Effects of a resistive barrier. *Biophys. J.* 45:1017–1025.

Kamiyama, A., K. Eguchi, and R. Shibayama. 1986. Circus movement tachycardia induced by a single premature stimulus on the ventricular sheet—evaluation of the leading circle hypothesis in the canine ventricular muscle. *Jpn. Circ. J.* 50:65–73.

Kienzle, M. G., R. C. Tan, B. M. Ramza, M. L. Young, and R. W. Joyner. 1987. Alterations in Endocardial activation of the canine papillary muscle early and late after myocardial infarction. *Circulation* 76:860–874.

Kim, S. S., R. Lal, and R. Ruffy. 1987. Paroxysmal nonreenstrant supraventricular tachycardia due to simultaneous fast and slow pathway conduction in dual atrioventricular node pathways. *J. Am. Coll. Cardiol.* 10:456–461.

Lazzara, R. 1988. Electrophysiological mechanisms for ventricular arrhythmias. *Clin. Cardiol.* :II 1–4.

Lazzara, R., and B. J. Scherlag. 1988. Generation of arrhythmias in myocardial ischemia and infarction. *Am. J. Cardiol.* 61:20A–26A.

Lesh, M. D., M. Pring, and J. F. Spear. 1989. Cellular uncoupling can unmask dispersion of action potential duration in ventricular myocardium. A computer modeling study. *Circ. Res.* 65:1426–1440.

Lin, F. C., S. J. Yeh, and D. Wu. 1985. Determinants of simultaneous fast and slow pathway conduction in patients with dual atrioventricular nodal pathways. *Am. Heart J.* 109:963–970.

Mahmud, R., S. T. Denker, M. H. Lehmann, A. Addas, and M. Akhtar. 1985. Unidirectional retrograde atrioventicular nodal block in man: determinants of reversibility by vagal antagonism. *Am. Heart J.* 110:568–574.

Mazgalev, T., L. S. Dreifus, J. Bianchi, and E. L. Michelson. 1981. The mechanism of AV junctional reentry: role of the atrionodal junction. *Anal. Rec.* 201:179–188.

Moe, G. K., C. Mendez, and J. Han. 1965. Aberrant A-V impulse propagation in the dog heart: a study of functional bundle branch block. *Circ. Res.* 16:261–286.

Moe, G. K., J. B. Preston, and H. Burlington. 1956. Physiologic evidence for a dual A-V transmission system. *Circ. Res.* 4:357–375.

Okumura, K., R. W. Henthorn, A. E. Epstein, V. J. Plumb, and A. L. Waldo. 1985. Further observations on transient entrainment: importance of pacing site and properties of the components of the reentry circuit. *Circulation.* 72:1293–1307.

Overholt, E. D., R. W. Joyner, R. D. Veenstra, D. Rawling, and R. Wiedmann. 1984. Unidirectional block between Purkinje and ventricular layers of papillary muscles. *Am. J. Physiol.* 247:H584–595.

Pressler, M. L. 1984. Cable analysis in quiescent and active sheep purkinje fibres. *J. Physiol.* 352:739–757.

Quan, W., anD Y. Rudy. 1990. Unidirectional block and reentry of cardiac excitation: a model study. *Circ. Res.* 66:367–382.

Reddy, C. P., and M. Lynch. 1978. Abolition and modification of reentry within the His-Purkinje system by procainamide in man. *Circulation.* 58:1010–1022.

Salerno, J. A., L. Tavazzi, M. Chimienti, M. Ray, and P. Bobba. 1979. Paroxysmal atrioventricular tachycardia involving an anomalous pathway with antegrade unidirectional block. *Eur. J. Cardiol.* 9:285–305.

Smith, J. M., and R. J. Cohen. 1984. Simple finite-element model accounts for wide range of cardiac dysrhythmias. *Proc. Natl. Acad. Sci. USA.* 81:233–237.

Tan, R. C., and R. W. Joyner. 1990. Electrotonic influences on action potentials from isolated ventricular cells. *Circ. Res.* 67:1071–1081.

Ursell, P. C., P. I. Gardner, A. Albala, J. J. Fenoglio, and A. L. Wit. 1985. Structural and electrophysiological changes in the epicardial border zone of canine myocardial infarcts during healing. *Circ. Res.* 56:436–451.

Wald, R. W., M. B. Waxman, and E. Downar. 1980. The effect of antiarrhythmic drugs on depressed conduction and unidirectional block in sheep Purkinje fibers. *Circ. Res.* 46:612–619.

Watanabe, Y. 1981. Effects of calcium and sodium concentrations on atrioventricular conduction: experimental study in rabbit hearts with clinical implications on heart block and slow calcium channel blocking agent usage. *Am. Heart J.* 102:883–891.

Waxman, M. B., E. Downar, and R. W. Wald. 1980. Unidirectional block in Purkinje fibers. *Can. J. Physiol. Pharmacol.* 58:925–933.

Weingart, R., and P. Maurer. 1988. Action potential transfer in cell pairs isolated from adult rat and guinea pig ventricles. *Circ. Res.* 63:72–80.